Chemical Science

EDGE ARTICLE

Check for updates

Shearing-induced formation of Au nanowires†

Yiwen Sun, [ab] An Su, [bc] Lecheng Zhao, [a] Xiaobin Liu, [ab] Xueyang Liu, [a] Yawen Wang [ID] *[a] and Hongyu Chen [ID] *[bc]

Shearing-induced nucleation is known in our daily lives, yet rarely discussed in nano-synthesis. Here, we demonstrate an unambiguous shearing-induced growth of Au nanowires. While in static solution Au would predominately deposit on pre-synthesized triangular nanoplates to form nano-bowls, the introduction of stirring or shaking gives rise to nanowires, where an initial nucleation could be inferred. Under specific growth conditions, CTAB is responsible for stabilizing the growth materials and the resulting oversaturation promotes shearing-induced nucleation. At the same time, all Au surfaces are passivated by ligands, so that the growth materials are diverted to relatively fresher sites. We propose that the different degrees of "focused growth" in active surface growth could be represented by watersheds of different slopes, so that the subtle differences between neighbouring sites would set course to opposite pathways, with some sites becoming ever more active and others ever more inhibited. The shearing-induced nuclei, with their initially ligand-deficient surface and higher accessibility to growth materials, win the dynamic inter-particle competition against other sites, explaining the dramatic diversion of growth materials from the seeds to the nanowires.

Introduction

Nucleation is the initial process in the formation of a crystal from a solution.[1–3] Controlling nucleation is of critical importance for modulating the crystallinity, size, and shape of crystals, which are important for the pharmaceutical industry, metallurgy, materials sciences, and beyond.[4,5]

Nucleation can be classified as either homogeneous or heterogeneous nucleation.[6] The latter refers to the formation of nuclei on the surface of a different phase, for example, dust particles, the wall of containers, or preexisting crystals as "seeds". The former refers to the formation of nuclei in a supersaturated solution without external assistance. It typically involves a higher "activation barrier" than heterogeneous nucleation, because the initial gathering of growth materials for making a nucleus is less favourable (forming fewer bonds) than attaching the growth materials to an existing surface.[7–11]

In addition to these two types of nucleation, shearing-induced nucleation is less known, but not uncommon in our daily lives. For example, an undisturbed super-cooled solution can remain liquid indefinitely, but upon shaking or knocking the container, it would quickly freeze into an icy block.[12] By inference, shearing is certainly involved in the nucleation of ice, although the nucleation process is difficult to characterize. However, the shearing solution cannot be defined as an interface between different phases, at least not in conventional terms.

In the literature, most of the studies on shearing-induced nucleation are based on computational simulation. The conclusions vary, as some believe that shearing can promote the rate of nucleation,[13] whereas others believe that shearing would inhibit nucleation.[14,15] There is no monotonic relationship between shearing rates and nucleation rates, with the maximum typically occurring somewhere in the middle.[16–19]

In terms of experimental studies, stirring has been found to play important roles,[15,20–23] for example, in affecting the TiO_2 nanocrystal morphology[21] and in lowering the reaction temperature and time for $BaTiO_3$ nanowires.[22] While it is obvious that stirring promotes material exchange in the solution, it is non-trivial regarding how the shearing induces nucleation and growth of crystals. More recently, shear flow was designed to promote the growth rate and crystal size of a variety of crystals, where shearing is believed to cause disentanglement of the surface ionic polymers, and thus promote nucleation and growth.[23]

In this work, we solve a long-standing puzzle that certain nano-synthesis reactions should not be shaken or stirred because of shearing-induced nucleation. We demonstrate unambiguous examples: in a static solution, growth occurs on

[a]Institute of Advanced Synthesis (IAS) and School of Chemistry and Molecular Engineering, Jiangsu National Synergetic Innovation Centre for Advanced Materials, Nanjing Tech University, Nanjing, 211816, China. E-mail: ias_ywwang@njtech.edu.cn

[b]Department of Chemistry, School of Science and Key Laboratory for Quantum Materials of Zhejiang Province, Research Center for Industries of the Future, Westlake University, Hangzhou 310030, P. R. China. E-mail: chenhongyu@westlake.edu.cn

[c]Institute of Natural Sciences, Westlake Institute for Advanced Study, Hangzhou 310024, China

seeds, but shaking (with an orbital shaker), stirring and other types of shearing, surprisingly, cause the formation of Au nanowires. The discovery was made under active surface growth conditions,[6,24] where Au deposition preferentially occured on sites with fewer ligands and the competition among different sites of each nanoparticle led to abnormal morphologies (e.g., Au nano-bowls).[25] In a shearing solution, new nuclei are formed independent of the seeds, and their initial fresh surface (with fewer ligands) and higher accessibility to growth materials help them win the inter-particle competition for growth materials, giving Au nanowires with more extensive growth than the active ridges on the seeds.

Results and discussion

Under typical conditions for synthesizing nano-bowls,[25] the seed solution with triangular Au nanoplates was added into a mixed solution containing the Au precursor $HAuCl_4$ (0.15 mM), the mixed ligands cetyltrimethylammonium bromide (CTAB, 9.8 mM) and L-cysteine (0.08 mM), and the reductant L-ascorbic acid (0.33 mM) under vigorous vortexing at 60 °C. The

difference is in the application of shearing: the uniformly mixed solution was then put in a 300 rounds per min (rpm) orbital shaker at 60 °C for 30 min. The products were then isolated and purified repeatedly before being subjected to microscopy characterization.

Fig. 1a and b show the scanning electron microscopy (SEM) images of a set of control experiments without and with shearing. The products obtained without shearing are nano-structures with a hexagonal outline (Fig. 1a); and with shearing, nanowires would form in addition to the hexagonal species (Fig. 1b and S1a†). The hexagonal nanostructures havetypes: an average edge length of 190 nm, and each of them has a distinctive triangular hump that encloses a concave centre. From the occasionally tilted particles (Fig. S2†), it can be observed that these hexagonal nanostructures have a plate-like morphology, with an average thickness of 86 nm. The hexagonal nanostructures are thus expected to arise from the seeds (Fig. S3†), which are triangular with an average edge length of 150 nm and thickness of 8 nm, after horizontal expansion and non-uniform vertical growth. The nanowires, which account for around 37% of the total nanostructures (based on the survey of
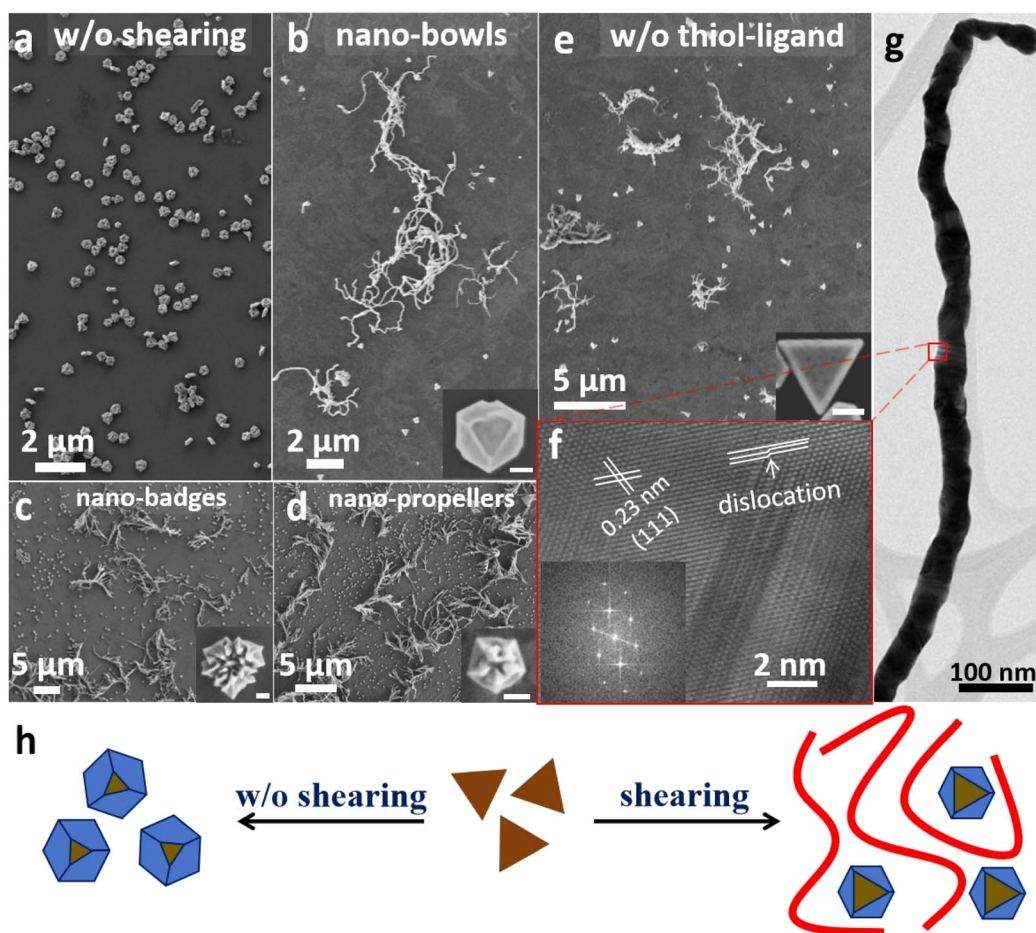

Fig. 1 SEM images of (a) nano-bowls in the absence of shearing and (b)–(e) Au nanowires as a by-product when shearing was applied during the syntheses of (b) nano-bowls,[25] (c) nano-badges,[27] (d) nano-propellers,[26] and (e) the same as (b), but in the absence of any thiol-based ligands. (f) HRTEM and (g) TEM images of the Au nanowires formed in (b). (h) Schematic illustrating the products in the synthesis of nano-bowls with shaking and without shaking.

over 1500 particles/nanowires, same below), have an average length of 7.0 μm and an average width of 57 nm. Given that the nanowires are not connected to the nano-bowls, it is likely that they originated from a homogeneous nucleation event during the growth process. In other words, while the homogeneous nucleation cannot be directly observed, it must have occurred to account for the formation of nanowires. Repeated experiments confirmed that without shearing, the same reaction conditions did not give nanowires.

Overall, the Au nanowires are wavy and sometimes entangled. The magnified transmission electron microscopy (TEM) images reveal that they have rugged surfaces with slightly variable diameters (Fig. 1g), as if they are made of jointed segments. High resolution TEM (HRTEM) images confirm that the nanowires are polycrystalline, and that the nanowire axis does not follow any specific crystalline orientation (Fig. 1f). Instead, there are numerous *fcc* domains and grain boundaries on each nanowire. Defects like stacking faults are common in each domain, and sometimes, the nanowires even bend and twist through a collection of twinning planes (Fig. S4†). Such structural characteristics suggest that the Au nanowires are formed through fast growth, so that many stacking mistakes are kinetically trapped.

The reaction parameters of the present system are the same as those in our previously reported synthesis of hexagonal nano-bowls,[25] yet the emergence of nanowires has completely deviated from the typical products. Such a difference is obviously caused by the additional shaking condition (Fig. 1h). The product obtained without shaking showed hexagonal nano-bowls with an edge length of 220 nm and thickness of 180 nm (Fig. 1a and S5a†), the same as those reported in our previous work. The hexagonal nanostructures as shown in the inset of Fig. 1b are the intermediates *en route* to the nano-bowls, as confirmed by time-dependent experiments (Fig. S6†). In other words, both the horizontal and vertical growth on the triangular nanoplate became much reduced after introducing the shaking condition, likely due to competition from the rapid growth of Au nanowires.

In comparison to the above-mentioned synthesis of nano-bowls using L-cysteine as the ligand, more recently, our group reported the room-temperature syntheses of chiral nano-badges[26] and nano-propellers[27] using L- and D-glutathione as ligands, under different reaction conditions including the use of Au decahedrons as seeds in the latter case. When we introduced the same shaking condition (300 rpm), Au nanowires were also obtained (Fig. 1c–d and S1b–c†), and the nano-badges and nano-propellers showed less extensive growth. Again, careful control experiments without shaking gave clean products without nanowires, with a high reproducibility (Fig. S5c and d†).

Other than competing for Au deposition, the presence of seeds has no obvious effect on the nanowire formation. Control experiments using spherical Au seeds (60 nm, Fig. S7†) or in the complete absence of seeds also gave Au nanowires of similar appearance (Fig. S8†). Nevertheless, without seeds it would be difficult to estimate the yield of Au nanowires. In our model studies, the triangular nanoplate seeds were used with the same

concentration, and thus, they serve as internal standards for accessing the relative degree of growth.

All the above systems contain both the weak CTAB and a strong thiol-based ligand cysteine or glutathione. Control experiments showed that similar Au nanowires could be obtained without the strong ligand (Fig. 1e and S1d†), though the triangular nanoplates in the background grew uniformly larger, without ridges and valleys. Hence, it appears that the shearing-induced growth of nanowires is quite general and inhibition by the strong ligand is not indispensable.

Indeed, the above method using a 300-rpm orbital shaker has already been optimized over extensive experiments. Shearing could also be introduced by other methods, with different forms and strengths that eventually affect the yield of nanowires. Similar Au nanowires were observed using magnetic stirring (1000 rpm), hand-shaking, or vortexing, giving 30.8%, 23.9%, and 19.3% Au nanowires, respectively (Fig. S9†). Among these methods, hand-shaking is arbitrary, consistent vortexing is difficult to achieve, and magnetic stirring involves a stir-bar and only affects the bottom of solution. Thus, in comparison, the orbital shaker can achieve the most uninformed shearing of solution. From the experimental results, it also gave the highest percentage of nanowires among all the methods we have tried.

The percentage of nanowires generally increased with the shaking rate. Few nanowires (2.3%) were observed at 50 rpm, and above 100 rpm, faster shaking rates led to a higher percentage of nanowires in the product (11.7–37%, Fig. S10†). A similar trend was observed with magnetic stirring: 100 rpm did not give nanowires, and above 150 rpm, the percentage of Au nanowires increased with higher stirring rates (1.5–33.2%, Fig. S11†). Such a positive correlation between the shaking/stirring rates and the percentage of nanowires in the product provides a strong support for shearing-induced nucleation (*vide infra*).

The above results show without ambiguity the enormous impact of shearing on nano-synthesis. In retrospect, many of the "failed" reactions in our previous attempts were probably due to serendipitous shaking or stirring, underscoring the importance of this discovery. In conventional wet-chemical synthesis, shaking or stirring is frequently used to help mixing, but no similar nanowire formation was reported, and other possible roles of such actions have rarely been discussed. It is important to note that nano-synthesis is particularly dependent on nucleation events, unlike molecular reactions. However, the transient nucleation is extremely difficult to characterize and has so far remained elusive.

It is known in the literature that a faster stirring rate gives rise to a stronger shear force in solution[21] and that shearing could promote both the collision frequency and the average kinetic energy of the monomers of growth materials.[28] Hence, the "hotspots" in a shearing solution could be viewed as equivalent to local high-temperature regions that increase the probability of nucleation, according to the Arrhenius equation. It follows that higher over-saturation would be more favourable for shearing-induced nucleation.

The direct result of shearing-induced nucleation would be ultrasmall nuclei that presumably compete in the growth to give

nanospheres, should there be no additional control. The formation of nanowires clearly involves symmetry breaking from the normal isotropic deposition to unidirectional growth, which requires additional explanation.

We carried out detailed analysis on CTAB first. In the absence of CTAB, the reduction of $HAuCl_4$ happened immediately after the addition of L-ascorbic acid, causing severe homogeneous nucleation and formation of Au nanoparticles with diameters around 40 nm (Fig. 2a and S12†). At 10% standard [CTAB] (0.98 mM), the same conditions as those in Fig. 1e gave very few (0.58%) Au nanowires (Fig. 2b), and the Au nanoplates grew into large irregular plates (400 nm width). They are much larger than the initial seeds (150 nm)[29] and the rugged edges should arise from growth[30] rather than etching.[31] The percentage of Au nanowires among nanoplates increased with [CTAB], with 11.4%, 15.9%, 37%, and 48.1% with 2.94 mM, 4.9 mM, 9.8 mM, and 29.4 mM CTAB, respectively (Fig. 2c–d and S13†). At the same time, the average length of the Au nanowires increased from 3.5 to 4.3, 7.0, and 8.1 μm, and there is a decrease in size for the Au nanoplates, indicating that an increasing amount of deposition occurred on the Au nanowires, as opposed to the original triangular nanoplates.

It is known that the Br^- ions of CTAB could coordinate to Au species, including Au^{3+}, Au^+, and the reduced form Au^0.[32] As such, [CTAB] was often modulated to control the rate of Au reduction.[33] In the presence of CTAB, the growth materials are well stabilized in the solution, to the degree that homogeneous nucleation remains inhibited even when the seed concentration is greatly reduced.[26,30] Judging from the rapid colour change in the above experiments with no CTAB or low [CTAB], insufficient stabilization is likely responsible for the quick Au deposition on the seeds.

When CTAB was replaced by its derivatives with various aliphatic chain lengths ($C_{12}TAB$, $C_{14}TAB$, $C_{16}TAB$ and $C_{18}TAB$), the percentage of Au nanowires among nanoplates increased monotonously in the series (0%, 6.3%, 37%, and 62%, respectively), with the average nanowire length in the last 3 cases being 4.2, 7.0, and >13.0 μm (Fig. 3 and S14†). Since the [Br^-]

and the head group were the same, the packing interaction among neighbouring ligands[34] should play a critical role in the nanowire formation.

The packing interaction increases with the aliphatic chain length, in the order: $C_{12}TAB < C_{14}TAB < C_{16}TAB < C_{18}TAB$. Thus, longer C_nTAB should be more effective in turning off the "old" sites and diverting growth to the "fresh" active sites. However, the packing interaction of C_nTAB is also known to affect the stabilization of solution Au species,[35,36] possibly via the formation of micelles. With more growth materials "hold-up" at the critical stage of nucleation, i.e., a higher degree of oversaturation, shearing can more effectively promote nucleation. Thus, the two effects of CTAB are corroborative.

In the case when C_nTAB derivatives with shorter chains ($n \leq 12$) did not give any Au nanowires (Fig. S15†), the stabilization effect appears to be too weak. This is a counterexample indicating that the oversaturation of the growth material (C_nTAB-stabilized Au^0 atoms) is a necessary condition for the initial shearing-induced nucleation.

In short, the main effect in Fig. 2 and 3 is that the higher [CTAB] and stronger C_nTAB packing shift growth materials from the nanoplate seeds to nanowires, likely by promoting shearing-induced nucleation (a higher percentage of nanowires) and
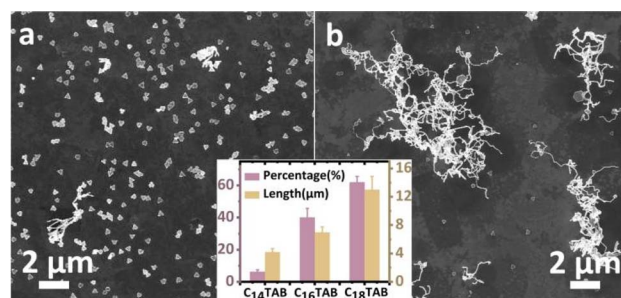

Fig. 3 SEM images of the products when the ligand $C_{16}TAB$ under the reaction conditions of Fig. 1d is changed to (a) $C_{14}TAB$ or (b) $C_{18}TAB$. Inset shows the histogram of the percentage of Au nanowires (purple) and their average length (orange).
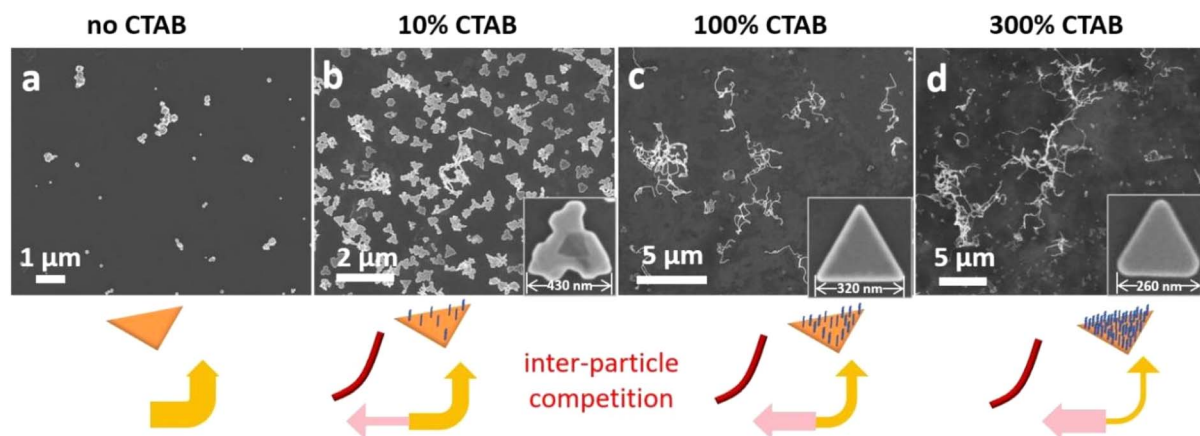

Fig. 2 Shifting of growth materials from the seeds to shearing-induced nanowires, when the [CTAB] was varied under the reaction conditions of Fig. 1d: SEM images of the products: (a) in the absence of CTAB; in the presence of (b) 10% standard [CTAB], (c) 100% [CTAB]; and (d) 300% [CTAB].

possibly also due to the preferential growth at the active sites (longer nanowires).

So far, the growth competition is between the seeds, which were grossly treated as "suppressed", and the nanowires, which presumably have at least one active tip per nanowire. Judging from the irregular shapes of nano-badges and nano-propellers, the deposition on the seeds was not uniform, with the more active sites forming ridges and the less active sites becoming valleys. If we define the competition among the active sites in each nanoparticle as "intra-particle competition", "inter-particle competition" would refer to competition for growth materials among the nanoparticles and nanowires. The former occurs under non-shearing conditions and has been previously reported. Thus, subsequently we focus our discussion on the inter-particle competition (Fig. 4).

There is an additional complexity: as shown in Fig. 4, during the synthesis of nano-badges in static solution and in the presence of glutathione,[26] there were occasional tails (1.4%) grown from and remained tethered to the nanoparticle. They were usually thinner, but longer (450–1200 nm) than the ridges (100–200 nm). The tails have clearly grown faster than the ridges, indicating that there are at least 3 levels of surface sites for the intra-particle competition (Fig. 4f): the valleys, the ridges, and the tails. With higher shearing (30 and 50 rpm orbital shakers), the percentage of nano-badges with tails increased to 6.4% and 8.2%, respectively. At 100 rpm (Fig. 4a) and 150 rpm, the number of wire-like structures increased obviously, but it is difficult to distinguish if they were all tethered to the nano-badges. At 300 rpm (Fig. 1c), the nanowires were much longer (average length 14 μm) and mostly untethered to the seeds.

Hence, there are 4 different levels of growth sites in the same reaction system, as shown in Fig. 4a, namely the valley sites, the ridge sites, the tethered tails, and the shearing-induced nanowires untethered to the seeds. They are related to each other but have different levels of activeness, which needs additional hypotheses.

There appears to be a correlation between the quality of crystallinity and the rate of growth: the nano-badges and nano-propellers were found to be nearly single-crystals, except for the twin defects inherited from the initial nanoplate seeds.[26,27] The nanowires, being the most active among the sites, were found with multiple grain boundaries and stacking faults, which are consistent with the rapidly grown nanowires from substrates.[37,38] Interestingly, the tails are between these two extremes: only about 25% of the tails contained stacking faults (Fig. S16†), consistent with their intermediate rate of growth.

The different levels of active sites have not been dealt with in our previous studies and are at the core of the shearing-induced formation of nanowires. An easy hypothesis is that the initial advantage of ligand deficiency, either by fresh nucleation or by serendipitous dissociation, may last long into the growth. However, the fact that all of the shearing-induced nuclei evolved into nanowires, as opposed to nanospheres (Fig. 5a), is strong evidence that part of their surface was quickly passivated. The formation of a wire shape requires constant inhibition at the side surface surrounding the emerging tip and thus, the small diameter of the tails and nanowires shows the rapid rate of inhibition. Control experiments also established that the nanowires stopped growing when shearing was stopped (Fig. S17†).

Previously, we have suggested that the "battleground" of active surface growth is not level:[30] the ligand-deficient sites are more active, and the constant growth refreshes their surface, making them ever more active, whereas the ligand-rich sites lose in the competition and become increasingly inhibited. To represent such a divergent growth mode, we draw a watershed (Fig. 5c): the biased battleground is the necessary condition for sustaining the initial fresh sites with constant growth, and it can even pick out tiny differences during random fluctuation (or sometimes patterned fluctuation[26]), and turn them into high-rising ridges. Without a watershed effect, the battleground is level, and the normal facet control takes over, with equivalent facets growing equivalently. In other words, when the rate of Au
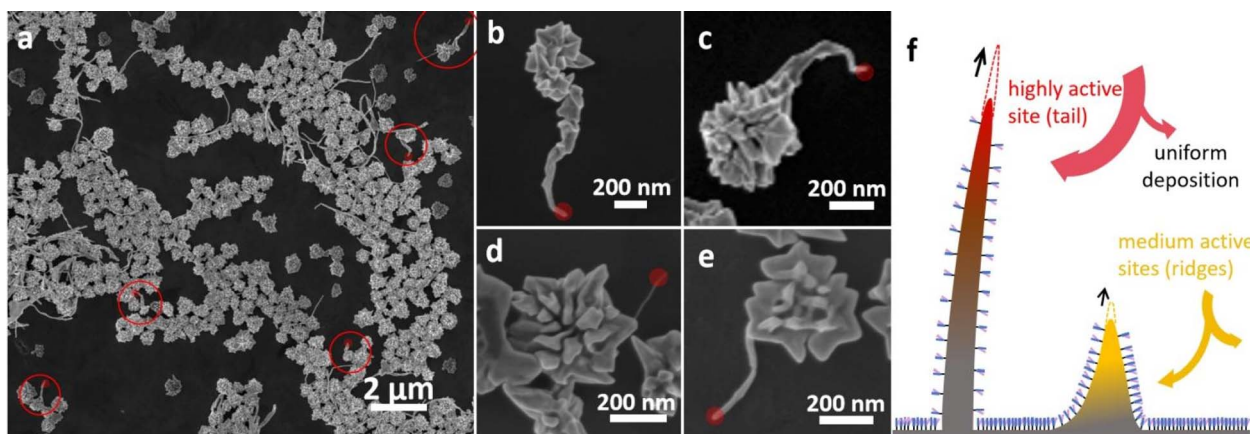

Fig. 4 A reaction system involves 4 different levels of activity: (a) SEM image of the Au nanowires and nano-badges obtained with a 100 rpm shaking rate; (b–e) typical tail-structures, either showing gradually smaller diameters as the advantages in activity were accumulated over time (b and c) or having uniform diameters, likely directly emerged by serendipity (d and e). (f) Schematics illustrating the intra-particle competition for growth materials, with different extents of focused growth at the ridges (medium active sites) or tails (highly active sites).
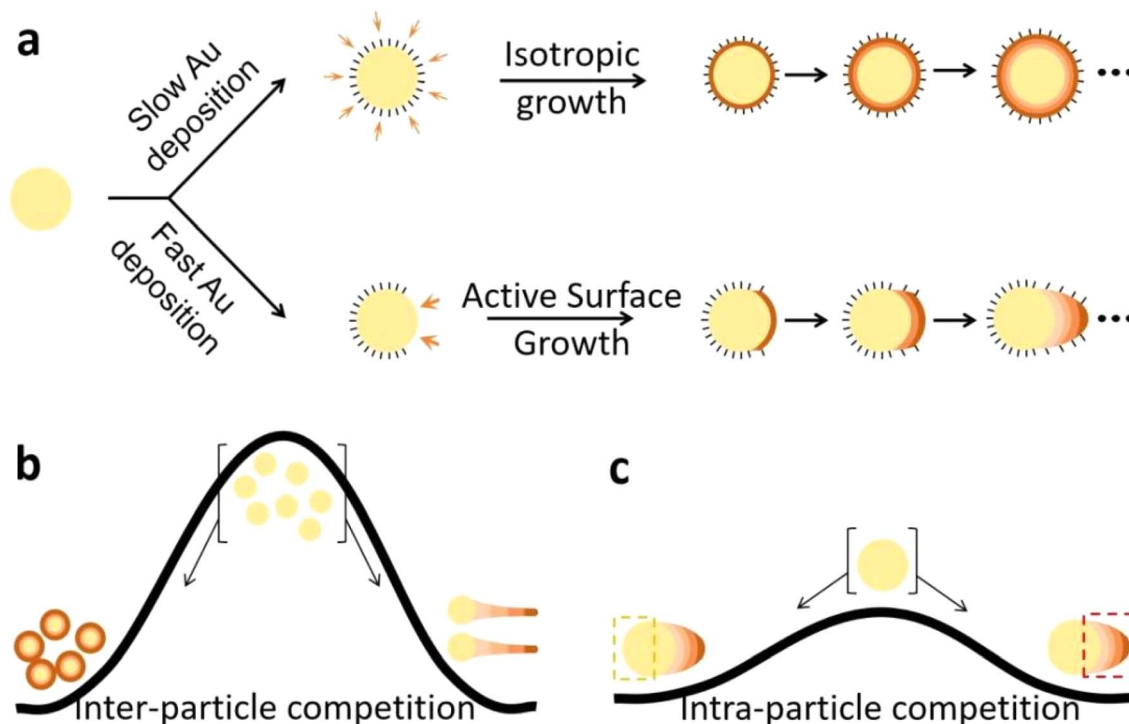
Fig. 5 (a) Schematic illustrating the difference between isotropic growth and active surface growth, where the non-uniform distribution of ligands is the direct reason for the focused growth at the active sites. (b and c) Schematics illustrating the difference between inter-particle and intra-particle competition, where the different slopes of watersheds represent the extent of divergent growth sustaining the active surface growth, with ever more inhibited sites at the left and ever more active sites at the right.

deposition is slower than the dynamics of ligand dissociation/association,[30] the lack of growth materials cannot sustain the active sites, and ligand passivation would remove the watershed effect.

The dynamic competition among various sites is likely achieved *via* the depleted concentration gradient of growth materials surrounding each site (the depletion sphere mechanism).[39] The scarcity of growth materials and overlapping depletion spheres could explain the relatively equal growth of the ridges on each nanoparticle. On this basis, we expect that short-distance intra-particle competition (among active ridges) should be fiercer and thus more equal than long-distance inter-particle competition (*i.e.*, between seeds and nanowires).

Our previous studies on active surface growth have established that the promoting factors are the strength of ligands (stronger anchoring bond, stronger packing, or higher ligand concentration) and the rate of material deposition (faster chemical reduction or fewer seeds). The above results have shown that inter-particle competition and shearing/mixing could also increase the rate of Au deposition.

To link these concepts and represent the different extents of divergent growth, we draw a watershed for the inter-particle competition (Fig. 5b) to have a steeper slope than that of intra-particle competition (Fig. 5c). The occasional tails could be viewed as the result of the intermediate level of the watershed between the two extremes (Fig. 4f), where the advantages could be accumulated over time (Fig. 4b and c) or directly emerged by serendipity (Fig. 4d and e). Their extra distance from the ridges

is critical for breaking free of the local competition and sustaining the initial advantage.

On this note, the different extents of "focused growth" in our previous studies could be represented by watersheds of different slopes. In the current work, the active sites occur in the same system with identical ligand conditions and reduction rates, and hence, the accessibility to growth materials becomes the main difference. Thus, inter-particle competition explains why most of the growth was shifted to the newly formed nanowires, especially under higher [CTAB] and longer C_nTAB conditions.

Conclusions

In summary, this work establishes the unambiguous difference between reactions with and without shearing. Shearing promotes the probability of nucleation, by causing local "hot-spots" with higher collision frequency and average kinetic energy, and the effects would be enhanced with higher over-saturation of growth materials.

CTAB is responsible for holding up the high over-saturation by stabilizing Au species, in a way similar to the hold-up of super-cooled conditions with ultraclean water, so that shearing could induce quick freezing. As a counterexample, insufficient [CTAB] or short C_nTAB cannot achieve high over-saturation and the growth materials are "leaked" by homogeneous nucleation. Similarly, without CTAB, thiol-based ligands can achieve neither active surface growth nor shearing-induced nucleation.

Both CTAB and thiol-based ligands dynamically passivated all Au surfaces, including the existing seed surface and the newly emerging active surface, so that the growth materials are diverted to the relatively fresher sites. The relative activity of different sites can be represented by watersheds of different slopes. Slight differences in growth conditions set the course for divergent growth, with some sites becoming ever more active and others becoming ever more inhibited. The shearing-induced nanowires, being more accessible to growth materials, could be understood as an extreme version of active surface growth on the seeds.

In the current system, CTAB is indispensable due to its role in stabilizing Au over-saturation and promoting active surface growth. Nevertheless, the formation of nanowires, by inference, provides important insights into the shearing-induced nucleation. Moreover, it explains the mysteriously failed experiments and also provides a unique perspective on the active surface growth mechanism.

Data availability

All data (experimental procedures and characterizations) are available within the article and the ESI.†

Author contributions

H. C. and Y. W. designed and supervised the project. Y. S carried out most of the experimental work and statistical analysis. H. C. and Y. W. conducted the mechanistic analysis and interpretations. A. S. provided advice on the role of CTAB and literature references. L. Z. and X. L. provided assistance with SEM, TEM and HRTEM characterization. All authors participated in the writing of the manuscript.

Conflicts of interest

The authors declare no conflict of interest.

Acknowledgements

Notes and references

1 D. Mordehai, O. David and R. Kositski, Nucleation-Controlled Plasticity of Metallic Nanowires and Nanoparticles, *Adv. Mater.*, 2018, **30**, 1706710.

2 J. Lee, J. Yang, S. G. Kwon and T. Hyeon, Nonclassical nucleation and growth of inorganic nanoparticles, *Nat. Rev. Mater.*, 2016, **1**, 16034.

3 J. F. Lutsko, How crystals form: a theory of nucleation pathways, *Sci. Adv.*, 2019, **5**, 7399.

4 X. Li, J. Wang, T. Wang, N. Wang, S. Zong, X. Huang and H. Hao, Molecular mechanism of crystal nucleation from solution, *Sci. China: Chem.*, 2021, **64**, 1460–1481.

5 K.-J. Wu, E. C. M. Tse, C. Shang and Z. Guo, Nucleation and growth in solution synthesis of nanostructures – from fundamentals to advanced applications, *Prog. Mater. Sci.*, 2022, **123**, 100821.

6 R. Xiao, J. Jia, R. Wang, Y. Feng and H. Chen, Strong Ligand Control for Noble Metal Nanostructures, *Acc. Chem. Res.*, 2023, **56**, 1539–1552.

7 A. Khaleghi, S. M. Sadrameli and M. Manteghian, Thermodynamic and kinetics investigation of homogeneous and heterogeneous nucleation, *Rev. Inorg. Chem.*, 2020, **40**, 167–192.

8 Y.-S. Jun, Y. Zhu, Y. Wang, D. Ghim, X. Wu, D. Kim and H. Jung, Classical and Nonclassical Nucleation and Growth Mechanisms for Nanoparticle Formation, *Annu. Rev. Phys. Chem.*, 2022, **73**, 453–477.

9 J. Li and F. L. Deepak, *In Situ* Kinetic Observations on Crystal Nucleation and Growth, *Chem. Rev.*, 2022, **122**, 16911–16982.

10 Y. Xiao, J. Wang, X. Huang, H. Shi, Y. Zhou, S. Zong, H. Hao, Y. Bao and Q. Yin, Determination Methods for Crystal Nucleation Kinetics in Solutions, *Cryst. Growth Des.*, 2017, **18**, 540–551.

11 A. S. Myerson and B. L. Trout, Nucleation from Solution, *Science*, 2013, **341**, 855.

12 R. Hu, C. Zhang, X. Zhang and L. Yang, Research status of supercooled water ice making: a review, *J. Mol. Liq.*, 2022, **347**, 118334.

13 R. S. Graham and P. D. Olmsted, Coarse-Grained Simulations of Flow-Induced Nucleation in Semicrystalline Polymers, *Phys. Rev. Lett.*, 2009, **103**, 115702.

14 R. Blaak, S. Auer, D. Frenkel and H. Löwen, Homogeneous nucleation of colloidal melts under the influence of shearing fields, *J. Phys.: Condens. Matter*, 2004, **16**, S3873–S3884.

15 Y. L. Wu, D. Derks, A. v. Blaaderen and A. Imhof, Melting and crystallization of colloidal hard-sphere suspensions under shear, *Proc. Natl. Acad. Sci. U. S. A.*, 2009, **106**, 10564–10569.

16 B. Lander, U. Seifert and T. Speck, Crystallization in a sheared colloidal suspension, *J. Chem. Phys.*, 2013, **138**, 224907.

17 D. Richard and T. Speck, The role of shear in crystallization kinetics: from suppression to enhancement, *Sci. Rep.*, 2015, **5**, 14610.

18 J. J. Cerdà, T. Sintes, C. Holm, C. M. Sorensen and A. Chakrabarti, Shear effects on crystal nucleation in colloidal suspensions, *Phys. Rev. E*, 2008, **78**, 031403.

19 P. Holmqvist, M. P. Lettinga, J. Buitenhuis and J. K. G. Dhont, Crystallization Kinetics of Colloidal Spheres under Stationary Shear Flow, *Langmuir*, 2005, **21**, 10976.

20 J. Liu and Å. C. Rasmuson, Influence of Agitation and Fluid Shear on Primary Nucleation in Solution, *Cryst. Growth Des.*, 2013, **13**, 4385–4394.

21 Y. Tang, Y. Zhang, J. Deng, J. Wei, H. L. Tam, B. K. Chandran, Z. Dong, Z. Chen and X. Chen, Mechanical Force-Driven Growth of Elongated Bending TiO_2-based Nanotubular Materials for Ultrafast Rechargeable Lithium Ion Batteries, *Adv. Mater.*, 2014, **26**, 6111–6118.

22 B. Xie, H. Zhang, H. Kan, S. Liu, M.-Y. Li, Z. Li, S. Zhu, S. Qiu and S. Jiang, Mechanical force-driven growth of elongated $BaTiO_3$ lead-free ferroelectric nanowires, *Ceram. Int.*, 2017, **43**, 2969–2973.

23 J.-K. Sun, Y. I. Sobolev, W. Zhang, Q. Zhuang and B. A. Grzybowski, Enhancing crystal growth using polyelectrolyte solutions and shear flow, *Nature*, 2020, **579**, 73–80.

24 Y. Feng, Y. Wang, J. He, X. Song, Y. Y. Tay, H. H. Hng, X. Y. Ling and H. Chen, Achieving Site-Specificity in Multistep Colloidal Synthesis, *J. Am. Chem. Soc.*, 2015, **137**, 7624–7627.

25 S. Yang, Y. Zheng, G. He, M. Zhang, H. Li, Y. Wang and H. Chen, From flat to deep concave: an unusual mode of facet control, *Chem. Commun.*, 2022, **58**, 6128–6131.

26 Y. Zheng, Q. Wang, Y. Sun, J. Huang, J. Ji, Z. J. Wang, Y. Wang and H. Chen, Chiral Active Surface Growth *via* Glutathione Control, *Adv. Opt. Mater.*, 2023, **11**, 2202858.

27 Y. Zheng, X. Li, L. Huang, X. Li, S. Yang, Q. Wang, J. Du, Y. Wang, W. Ding, B. Gao and H. Chen, Homochiral Nano-propeller *via* Chiral Active Surface Growth, *J. Am. Chem. Soc.*, 2024, **146**, 410–418.

28 A. Goswami and J. K. Singh, Homogeneous nucleation of sheared liquids: advances and insights from simulations and theory, *Phys. Chem. Chem. Phys.*, 2021, **23**, 15402–15419.

29 Y. Huang, A. R. Ferhan, Y. Gao, A. Dandapat and D.-H. Kim, High-yield synthesis of triangular gold nanoplates with improved shape uniformity, tunable edge length and thickness, *Nanoscale*, 2014, **6**, 6496–6500.

30 Y. Zheng, J. Zong, T. Xiang, Q. Ren, D. Su, Y. Feng, Y. Wang and H. Chen, Turning weak into strong: on the CTAB-induced active surface growth, *Sci. China: Chem.*, 2022, **65**, 1299–1305.

31 B. He, Y. Wang, M. Zhang, Y. Xu, Y. Zheng, X. Liu, H. Wang and H. Chen, Serrated Au Nanoplates *via* the Sharpening Etching Mode, *Chem. Mater.*, 2022, **34**, 8213–8218.

32 J. Mosquera, D. Wang, S. Bals and L. M. Liz-Marzán, Surfactant Layers on Gold Nanorods, *Acc. Chem. Res.*, 2023, **56**, 1204–1212.

33 K. Kurihara, J. Kizling, P. Stenius and J. H. Fendler, Laser and pulse radiolytically induced colloidal gold formation in water and in water-in-oil microemulsions, *J. Am. Chem. Soc.*, 1983, **105**, 2574.

34 Y. Wang, J. He, C. Liu, W. H. Chong and H. Chen, Thermodynamics *versus* Kinetics in Nanosynthesis, *Angew. Chem., Int. Ed.*, 2014, **54**, 2022–2051.

35 J. Pérez-Juste, L. M. Liz-Marzán, S. Carnie, D. Y. C. Chan and P. Mulvaney, Electric-Field-Directed Growth of Gold Nanorods in Aqueous Surfactant Solutions, *Adv. Funct. Mater.*, 2004, **14**, 571–579.

36 J. Rodríguez-Fernández, J. Pérez-Juste, P. Mulvaney and L. M. Liz-Marzán, Spatially-Directed Oxidation of Gold Nanoparticles by Au(III)–CTAB Complexes, *J. Phys. Chem. B*, 2005, **109**, 14257–14261.

37 Y. Wang, J. He, X. Mu, D. Wang, B. Zhang, Y. Shen, M. Lin, C. Kübel, Y. Huang and H. Chen, Solution Growth of Ultralong Gold Nanohelices, *ACS Nano*, 2017, **11**, 5538–5546.

38 X. Wu, H. Li, W. Wang, D. Su, X. Wang, X. Tao, Y. Wang and H. Chen, Template-less Synthesis of Coded Au Nanowires, *Nano Lett.*, 2021, **21**, 1156–1160.

39 Y. Feng, Y. Wang, X. Song, S. Xing and H. Chen, Depletion sphere: explaining the number of Ag islands on Au nanoparticles, *Chem. Sci.*, 2017, **8**, 430–436.